

## Maximum Smoke Temperature in Non-Smoke Model Evacuation Region for Semi-Transverse Tunnel Fire

B. Lou<sup>1</sup>, Y. Qiu<sup>1†</sup> and X. Long<sup>2</sup>

<sup>1</sup> School of Electric Power, South China University of Technology, Guangzhou, Guangdong Province, 510640, China

<sup>2</sup> School of Chemistry and Chemical Engineering South China University of Technology, Guangzhou, Guangdong Province, 51064, China

†Corresponding Author Email: [qiu.yonghai@qq.com](mailto:qiu.yonghai@qq.com)

(Received May 10, 2016; accepted February 25, 2017)

### ABSTRACT

Smoke temperature distribution in non-smoke evacuation under different mechanical smoke exhaust rates of semi-transverse tunnel fire were studied by FDS numerical simulation in this paper. The effect of fire heat release rate (10MW 20MW and 30MW) and exhaust rate (from 0 to 160m<sup>3</sup>/s) on the maximum smoke temperature in non-smoke evacuation region was discussed. Results show that the maximum smoke temperature in non-smoke evacuation region decreased with smoke exhaust rate. Plug-holing was observed below the smoke vent when smoke exhaust rate increased to a certain value. Smoke spreading distance can be divided into three stages according to changes of smoke exhaust rate. The maximum smoke temperature model concluded that the peak temperature rise at tunnel vault is proportional to 0.75 power of dimensionless fire power. The maximum temperature in non-smoke evacuation region decays exponentially with the increase of smoke exhaust rate. However smoke vent interval influences the dimensionless maximum temperature in non-smoke evacuation region slightly. Smoke vent interval influences the dimensionless maximum temperature in non-smoke evacuation region slightly.

**Key words:** Tunnel fire; Semi-transverse ventilation; Plug-holing; Temperature distribution.

### NOMENCLATURE

$c_p$	specific heat at constant pressure	$\dot{m}$	smoke mass flow rate generated by fire accident
$C_s$	smagorinsky constant (LES)	$p$	on behalf of the full-size model
$D$	contact perimeter between smoke and tunnel	$Pr$	Prandtl number
$D^*$	characteristic length of fire source	$Q$	fire power
$Fr$	froude number	$Sc$	Schmidt number
$g$	acceleration of gravity	$T_0$	environmental temperature
$H$	distance from flame surface to tunnel vault	$T_{v,max}$	the maximum smoke temperature in the non-smoke evacuation region when smoke exhaust rate is $v$ , K
$H_1$	discharge flue height, m	$u$	ventilation velocity
$K_1$	an empirical constant	$v$	smoke exhaust rate
$K_2$	the flue gas temperature attenuation coefficient	$x$	the distance away from the fire source
$K_3$	temperature decline coefficient	*	dimensionless number
$l$	length	$\Delta T$	temperature difference
$L$	smoke spreading distance	$\rho_0$	environmental air density
$m$	on behalf of the small size model		

## 1. INTRODUCTION

High-temperature smoke generated by tunnel fire hazard destroys the tunnel structure and its toxic components threaten personnel security greatly (Jie *et al.* 2010). Related researches (Hu *et al.* 2008) reported that 85% casualties in tunnel fire hazard are caused by high-temperature toxic smoke. Therefore, it is very important to study the smoke spreading during tunnel fire. Due to the tunnel is semi-closed, heats and smoke generated by fire are difficult to be exhausted, good ventilation and smoke exhaust system design is vital to protect personnel security in tunnels.

Longitudinal ventilation system has a jet fan arranged in the vault of the tunnel, and when the fire occurs the jet fan is opened to prevent the flue gas from flowing back. Because of its simple design, it has advantage in economic and energy saving, less construction investment and low running cost. So many scholars have studied smoke temperature distribution, backflow distance and critical ventilation velocity when there's fire in longitudinal ventilation system (Jafari *et al.* 2011; Li *et al.* 2012; Zhang *et al.* 2012; Vauquelin and Y 2006; Hu *et al.* 2004; Hu and Huo 2008). Kurioka *et al.* (2003) use three kinds of model tunnels to study the fire phenomena in the near field of a fire in a tunnel and the aspect ratio of tunnel cross-section, heat release rate and longitudinal forced ventilation velocity were varied. Based on the study an empirical formulae for flame tilt, apparent flame height, maximum temperature of the smoke layer and its position were developed. K. Brahim *et al.* (2013) used the numerical tool FDS4.0 to carry out on a small scale tunnel model to study the fire-induced smoke control by longitudinal and longitudinal-natural ventilation systems. The results shows that the longitudinal velocity affects the thermal stratification especially and instability of stratification resulted in a strong mixing between the buoyant flow and the air flow, and thus a thickened buoyant smoke layer.

While longitudinal ventilation system also has obvious disadvantages that is security of workers and vehicles declined significantly in conditions of two-way traffic, traffic jam and secondary accidents. Semi-traverse ventilation system has a special smoke exhaust passage arranged at the top of the tunnel. When the fire occurs, the smoke is discharged through the exhaust port into the smoke exhaust passage, could discharge smoke effectively and control smoke within a short tunnel region where there's fire accident. It is increasingly applied in long tunnels. Therefore, it is significant to study smoke exhaust characteristics of tunnel fire in the semi-transverse ventilation system.

Many researches on smoke control in semi-traverse ventilation tunnel mainly focus on effects of smoke vent shape, interval and smoke exhaust rate on smoke exhaust efficiency (Vauquelin and Telle 2005; Lin and Chuah 2008; Choi 2005; Harish and Venkatasubbaiah 2014). Vauquelin and Telle (2005) carried out an experimental study on a reduced scale tunnel model to evaluate the longitudinal velocity

induced into a tunnel with two exhaust vents in tunnel fire. And a confinement velocity that was needed to prevent the smoke layer propagation downstream the vent was evaluated for several values. Ballesteros-TajaduraSantolaria-Morros and Blanco-Marigorta (2006) studied smoke spreading characteristics in the slope section of Inner Belt tunnel through FLUENT numerical simulation, finding that existing engineering designed smoke exhaust rate of draught fan couldn't discharge fire smoke effectively. Some smoke still could spread to downstream of the tunnel, and suggested that smoke vent shall be set at upslope of fire source and standard vent layout (smoke vents are set at two ends of fire source symmetrically) would reduce mechanical smoke evacuation efficiency significantly.

The exhaust vent position also has a great influence on the exhaust efficiency. Vauquelin (2002) analyzed effect of smoke vent location and shape on smoke exhaust efficiency of semi-traverse tunnel through a small experimental device. For the same shape and same area, a duct located at the ceiling is more efficient than a duct located in one of the walls and the location of the duct at the ceiling seems to have no significant influence. According to experimental result of Yi *et al.* (2015) smoke vent closer to fire source has higher smoke and heat exhaust efficiency and decreasing smoke vents is beneficial to increase smoke and heat exhaust efficiency. Vauquelin and Telle (2005) studied smoke backflow distance under different smoke exhaust rates through a small size experiment and proposed that smoke exhaust rate when smoke backflow is controlled within  $4H$  ( $H$  is tunnel height) behind the smoke vent is the full smoke exhaust rate and ventilation velocity in the tunnel caused by mechanical smoke exhaust is the "control velocity".

And the phenomenon of the plug-holing below the smoke vent is very special in the semi-transverse tunnel fire (Ji *et al.* 2012, Xu *et al.* 2013). Ji *et al.* (2012) carried out a set of burning experiments to investigate the effect of vertical shaft height on natural ventilation in tunnel fires. Two special phenomenon, plug-holing and turbulent boundary-layer separation were observed. The study found that with the increasing of shaft height the smoke layer separation becomes inconspicuous and the plug-holing occurs, leading to the ambient fresh air beneath smoke layer being exhausted directly. Therefore it is not the case that the higher vertical shaft, the better the smoke exhaust effect, there exist a critical shaft height. So that in this paper to study the critical smoke exhaust velocity to the best smoke exhaust effect point.

These researches have important significance to understand smoke exhaust law of ventilation system. In recent years, more attention on the study (Fan *et al.* 2013; Chow and Li 2011; Chow and Gao 2009) of tunnel fire is the smoke spread under the natural ventilation. Chen *et al.* (2015) reveals the effect of the distance between ceiling extraction (opening) distance and heat source on the thermally-driven smoke back-layering flow length beneath the ceiling in a tunnel with combination of ceiling extraction

and longitudinal ventilation. A new model is theoretically deduced to predict the smoke back-layering flow length including the factor of heat source-ceiling extraction (opening) distance, by accounting for the energy loss due to extraction which is calculated based on the local longitudinal temperature profile estimation.

The non-smoke evacuation region behind smoke vent is for escape and fire rescue. But only few researches on smoke spreading law and smoke temperature distribution in the non-smoke evacuation region have been reported yet. There are some theoretical and experimental researches on smoke temperature in semi-traverse tunnel. Wang and Zhu (2009) made a full-size experimental research on smoke spreading characteristics in tunnel under natural ventilation and established a formula to predict the maximum smoke temperature and smoke backflow distance. Kashef and Lei (2012) studied smoke temperature distribution and spreading distance at tunnel vault under natural ventilation through a small size experiment. Based on the one-dimensional theoretical model and dimensionless analysis and established two formulas to predict vault temperature distribution in flame area and non-flame area.

However, mechanical ventilation system plays the key role in smoke spreading control. This is different from natural ventilation conditions. In this paper, relationships between smoke temperature distribution, smoke spreading distance and maximum temperature in non-smoke evacuation region under semi-traverse ventilation system and smoke exhaust rate as well as fire power were explored by combing theoretical analysis and numerical simulation. A research method of smoke temperature in non-smoke evacuation region was put forward and a maximum smoke temperature prediction model was established.

## 2. THEORETICAL ANALYSIS OF INFLUENCING FACTORS

### 2.1 Free-Spreading Smoke Temperature Decline Model

He (1999) had put forward a longitudinal free-spreading smoke temperature decline formula for fire accident in horizontal tunnel:

$$\frac{\Delta T_x}{\Delta T_{\max}} = K_1 e^{-K_2} \quad (1)$$

Where  $\Delta T_x$  is the difference between smoke gas temperature at the place where is  $x$  away from the fire source and environmental temperature,  $\Delta T_{\max}$  is the maximum temperature difference between smoke gas and environment at the fire position;  $K_1$  is an empirical constant,  $K_2$  is the flue gas temperature attenuation coefficient, and then Hu *et al.* (2008) through theoretical analysis proposed  $K_2 = \alpha D / c_p \dot{m}$ , where  $\alpha$  is heat transfer coefficient;  $\dot{m}$  is smoke mass flow rate generated by fire accident;  $D$  is contact perimeter between smoke and tunnel;  $c_p$  is specific heat at constant pressure.

The maximum smoke temperature beneath the vault is related with fire power, natural ventilation velocity ( $u$ ) and flame surface height. For the maximum smoke temperature, Kurioka *et al.* (2003) made a series of small size experimental researches and proposed the empirical formula of maximum smoke temperature underneath the tunnel vault:

$$\frac{\Delta T_{\max}}{T_0} = \gamma \left( \frac{Q^{*2/3}}{Fr^{1/3}} \right)^\varepsilon \quad (2)$$

$$\left\{ \begin{array}{l} \frac{Q^{*2/3}}{Fr^{1/3}} < 1.35, \quad \gamma = 1.77, \quad \varepsilon = 6/5 \\ \frac{Q^{*2/3}}{Fr^{1/3}} \geq 1.35, \quad \gamma = 2.54, \quad \varepsilon = 0 \end{array} \right. \quad (3)$$

$$Q^* = Q / (\rho_0 c_p T_0 g^{1/2} H^{5/2}) \quad (4)$$

$$Fr = u^2 / (gH) \quad (5)$$

Where  $\rho_0$ ,  $T_0$ ,  $g$ ,  $c_p$ ,  $H$  are environmental air density, temperature, acceleration of gravity, specific heat at constant pressure and distance from flame surface to tunnel vault;  $u$  is ventilation velocity;  $Q^*$  is the characteristic fire power; and  $Fr$  is Froude number. According to above formulas, smoke temperature distribution in tunnel when there is no smoke evacuation could be expressed as:

$$T = f(Q, \rho_0, T_0, c_p, g, H, x, u, \nu) \quad (6)$$

### 2.2 Dimensionless Analysis of Smoke Temperature Under Semi-traverse Ventilation

Except for factors in Eq.(6), smoke spreading characteristics and vault smoke temperature distribution in semi-traverse ventilation tunnel are also related with smoke exhaust rate, smoke vent interval and shape. This paper paid key attentions to effect of smoke exhaust rate and fire power on smoke spreading in semi-traverse ventilation tunnel. Based on Eq.(6), smoke temperature can be expressed as a function of fire power ( $Q$ ), density ( $\rho_0$ ), environmental temperature ( $T_0$ ), specific heat at constant pressure ( $c_p$ ), acceleration of gravity ( $g$ ), tunnel height ( $H$ ), distance between survey point and fire source ( $x$ ), smoke exhaust rate ( $\nu$ ) and discharge flue height ( $H_1$ ).

$$T = f(Q, \rho_0, T_0, c_p, g, H, x, \nu, H_1) \quad (7)$$

Then, the calculation formula of dimensionless temperature is:

$$\frac{T}{T_0} = f(Q^*, \frac{x}{H}, \nu^*) \quad (8)$$

It reflects that the dimensionless temperature is related with characteristic fire power  $Q^* = Q / (\rho_0 T_0 c_p g^{1/2} H^{5/2})$ , characteristic fire source distance  $x/H$ , and the characteristic smoke exhaust rate  $\nu^* = \nu / \sqrt{gH_1}$ . When  $\nu^* = 0$ , Eq.(1) is the vault smoke temperature spreading and decline model under free ventilation conditions. Smoke temperature is only related with fire power and

distance to the fire source.

Combining Eq.(8) and (1), this paper made a numerical simulation on natural ventilation tunnel and forced smoke exhaust tunnel based on the vault smoke temperature spreading and decline model under free ventilation conditions and maximum smoke temperature in non-smoke evacuation region ( $T_{v0,max}$ ). Maximum smoke temperatures in non-smoke evacuation region under different smoke exhaust rates ( $T_{v,max}$ ) were gained. On the basis of dimensionless analysis and simulation results, semi-empirical relationship formula between  $T_{v0,max}$  and fire power as well as smoke exhaust rate was created.

### 3. NUMERICAL SIMULATION

Numerical simulation and experimental research is two of the most commonly method to study tunnel fire smoke spread features. Due to the high cost of full-scale experiment and the limitations of small size experiment to a certain extent, in recent years, with the booming development of computer technology and computational fluid dynamics calculation, many scholars began to do the numerical simulation study of the fire. Numerical simulation studies aimed at the fire smoke diffusion condition, temperature, wind speed and pressure distribution in tunnel. FDS (Fire Dynamics Simulator) simulation software is the product developed by American national standards institute (ANSI) building and fire research lab (BFRL). Its numerical method driven by the heat effect of low Mach number flow Navier - Stokes equations, focus on the calculation of fire smoke heat transfer process. Governing equations are described as follows:

Conservation of mass:

$$\frac{\partial \rho}{\partial t} + \Delta \rho \bar{u} = 0 \quad (9)$$

Conservation of momentum:

$$\rho \left( \frac{\partial \bar{u}}{\partial t} + \frac{1}{2} \Delta |\bar{u}|^2 - \bar{u} \times \omega \right) + \Delta P - \rho g = \bar{f} \cdot \sigma \quad (10)$$

Conservation of energy:

$$\frac{\partial (\rho h)}{\partial t} + \Delta \cdot (\rho h \bar{u}) = \frac{\partial P}{\partial t} + \bar{u} \cdot \Delta P - \Delta \bar{q}_r + \Delta \cdot (k \Delta T) + \Delta \cdot (k \Delta T) + \sum_i \Delta \cdot (h_i \rho D_i \Delta Y_i) \quad (11)$$

Conservation of species:

$$\frac{\partial}{\partial t} (\rho Y_i) + \Delta \cdot (\rho Y_i \bar{u}) = \Delta (\rho D_i \Delta Y_i) + m^{\cdot} \quad (12)$$

Ideal gas equation:

$$p_0 = \rho TR \sum_i (Y_i / M_i) \quad (13)$$

The FDS model consists of direct numerical simulation (DNS) and Large Eddy Simulation (LES). The direct simulation is directly solving the complete three-dimensional unsteady Navier-Stokes equations,

so the amount of calculation is very large LES is presented by Smagorinsky, the basic idea is to decompose the instantaneous motion of turbulence into two parts: scale (grid) motion and small scale (subgrid scale) motion. In the calculation of LES, many small vortices are used to describe the detail of the flow field, and only the large eddy motion is simulated. In recent years, the technology has achieved great success in dealing with complex turbulence and fire science. Hu *et al.* (2006) used FDS simulation to study the maximum smoke temperature under the ceiling in a tunnel fire and the predicted smoke temperatures were verified by comparing with the experimental measured value. Fairly good agreement was achieved. Lin and Li (2014) studied the influence of slope to half-and-half transverse ventilation tunnel fire smoke spread characteristic by using FDS numerical simulation. Lee and Ryou (2006) studied the influence of cross section ratio on tunnel fire smoke spread characteristics experimentally and numerically. Temperature distribution (using FDS3.0 simulation) under the ceiling showed a relatively good agreement with experimental results within 10 °C.

Many scholars study shows that it is feasible and effective by using FDS to study the characteristics of tunnel fire smoke spread and the temperature distribution. In this paper, a large eddy simulation model based on FDS was adopted. Definition of turbulent viscosity in FDS (McGrattan 2006):

$$\mu_{LES} = \rho (C_s \Delta)^2 [2 \bar{S}_{ij} : \bar{S}_{ij} - \frac{2}{3} (\Delta \cdot \bar{u})^2]^{\frac{1}{2}} \quad (14)$$

Where  $\Delta$  is the filter width, A is the volume of the cube root of grid,  $C_s$  is Smagorinsky constant, it varies in 0.1-0.25 with the changes of the flow field in different flow field. Other diffusion parameters, thermal conductivity and diffusivity are related to turbulent viscosity:

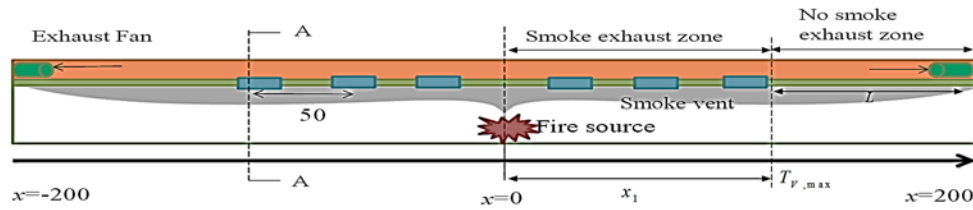
$$k_{LES} = \frac{\mu_{LES}}{Pr}, (\rho D) = \frac{\mu_{LES}}{Sc} \quad (15)$$

The turbulent Prandtl number (Pr) and Schmidt number (Sc) is constant. Since the FDS was released in 2000, a lot of verification experiments have been carried out to improve the reliability of FDS simulation. According to many previous experiments, it is shown that the constant  $C_s$ , Pr and Sc are set to 0.2, 0.5, and 0.5 respectively in FDS (McGrattan 2006).

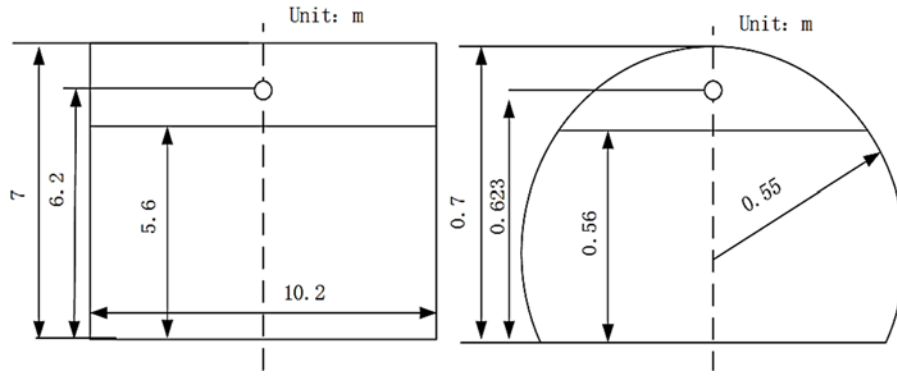
#### 3.1 Grid Division

In numerical simulation study, grid scale is a very important parameters. But in FDS large-eddy simulation (LES) model, grid scale in the simulation region must meet sub-grid scale (SGS) in order to calculate viscosity stress model of flow field accurately. Therefore, grid scale close to the fire source is generally determined by characteristic length of fire source ( $D^*$ )

$$D^* = \left( \frac{Q}{\rho_0 c_p T_0 g^{1/2}} \right)^{2/5} \quad (16)$$



a) Longitudinal distribution of the tunnel



b) Cross-section of Yi's small-scale model and full-scale model

**Fig. 1. Tunnel model.**

Where  $D^*$  is characteristic length of fire source, m;  $Q$  is fire power, kW;  $\rho_0$  is environmental density,  $\text{kg/m}^3$ ;  $c_p$  is specific heat at constant pressure,  $\text{kJ}/(\text{kg}\cdot\text{K})$ ;  $T_0$  is environmental temperature, K;  $g$  is acceleration of gravity,  $\text{m/s}^2$ .

McGrattan Baum and Rehm (1998) discovered that when grid scale is  $0.1D^*$ , the FDS LES simulation result agrees with the fitting curve of experiment. In this simulation, the minimum fire power was 10MW and  $D^*$  was calculated 2.5m. Grid scale was set  $0.1D^*$ , that is, 0.25m. Considering sizes of smoke vent and smoke exhaust fan, grid scale was determined  $0.24\text{m}\times 0.24\text{m}\times 0.24\text{m}$  in this paper. It was confirmed reasonable by the following study results

### 3.2 Tunnel Model and Reliability Verification

Due to the full-size experimental study on semi-traverse tunnel fire is very little, and to fire the buoyancy turbulence, smoke flow properties has nothing to do with the size (McCaffrey and Quintiere 1977). Yi *et al.* (2015) made a 1:10 small semi-traverse tunnel experiment to study effect of smoke vent area and interval on smoke and heat exhaust efficiency. Therefore the full-size simulation experiment is established by using the model experiment according to the principle of similar full-size simulation.

According to the  $Fr$  similarity criterion, the parameter model and the full size for similar relationship:

$$Fr = \frac{u_m^2}{gl_m} = \frac{u_p^2}{gl_p} \quad (17)$$

Where  $l$  is length (m),  $m, p$  on behalf of the small size and full-size model respectively. The relation of physical quantities based on  $Fr$  similarity principle represented as below:

$$\text{Temperature: } T_m / T_p = 1 \quad (18)$$

$$\text{Fire power: } Q_m / Q_p = (l_m / l_p)^{5/2} \quad (19)$$

$$\text{Volume flow-rate: } V_m / V_p = (l_m / l_p)^{5/2} \quad (20)$$

This paper established a full-scale tunnel model by using FDS (Fig. 1) based on Froude number similarity criterion. Size of this tunnel was  $400\text{m}$  ( $L$ )  $\times$   $10.2\text{m}$  ( $W$ )  $\times$   $7\text{m}$  ( $H$ ). The flue sheet was set 5.6m high from the ground and propylene carried in FDS was chosen as fuel. Smoke exhaust fans were installed at two sides of the discharge flue. T25 case in Yi's experiment was used as the control group to verify reliability of this simulation. The tunnel can be separated into two regions: smoke evacuation region from the fire source to the furthest distance of smoke vent ( $x_1$ ) and the non-smoke evacuation region from  $x_1$  to the tunnel exit. Since FDS is only applicable to establish model of regular boundary, arched tunnel was simulated through pileup of small rectangles. However, this caused sawtooth shape in the tunnel and vortex close to walls, which influenced simulation accuracy. Here, SAWTOOTH=FALSE. is employed in the FDS modeling to reduce sawtooth in the tunnel and improve flow condition close to walls. Table. 1 shows working conditions of Yi's small-scale experiment and our full-scale numerical simulation. Other boundary conditions were set same with the experiment.

In principle of similarity, temperature ratio of the

**Table 1 Working conditions of small-scale experiment based on Froude number similarity criterion and the full-scale simulation**

	fire power (kW)	Smoke exhaust rate (m <sup>3</sup> /s)	Smoke vent area (m <sup>2</sup> )	Smoke vent interval (m)	Number of opening smoke vents
Small-scale experiment	90	0.38	0.08	5	6
Full-scale simulation	30000	120	8	50	6

**Table 2 Result comparison between small-scale experiment and full-scale simulation**

	Smoke temperature at smoke vent(°C)			Temperature at fan exit(°C)	Heat exhaust efficiency of fan (%)	Total heat exhaust efficiency (%)
	L3	L2	L1			
Small-scale experiment	64.08	152.65	235.23	48.58	14.23	53.35
Full-scale simulation	68.25	142.13	248.8	48.2	13.6	51.8
Error(%)	-6.5	6.9	-5.4	0.78	4.5	3

**Table 3 Simulated working cases**

case	Fire power (MW)	Smoke exhaust rate (m <sup>3</sup> /s)	case	Fire power (MW)	Smoke exhaust rate (m <sup>3</sup> /s)	case	Fire power (MW)	Smoke exhaust rate (m <sup>3</sup> /s)
1	10	0	9	20	0	18	30	0
2	10	20	10	20	20	19	30	20
3	10	40	11	20	40	20	30	40
4	10	60	12	20	60	21	30	60
5	10	80	13	20	80	22	30	80
6	10	100	14	20	100	23	30	100
7	10	120	15	20	120	24	30	120
8	10	140	16	20	140	25	30	140
			17	20	180	26	30	160

full-scale model and the small-scale experiment is 1. Comparison results of simulation results and experimental results are shown in Table 2.

The result shows that small-scale experiment and full-scale simulation have similar temperatures at smoke vent and fan exit as well as smoke exhaust efficiency, showing a small error range (<10%). To study effect of fire power, smoke exhaust rate and smoke vent interval on smoke temperature in the non-smoke evacuation region, this paper used same tunnel model. Simulated working cases are listed in Table 3. The simulated fire power was 10MW~30MW, within the fire size range of different vehicle types suggested by NFPA (2010).

#### 4. RESULTS AND ANALYSIS

##### 4.1 Free-Spreading Smoke Temperature Distribution

Fig. 2 shows vault temperature distributions under working case 1, 8 and 16. It can be seen that the smoke temperature under the tunnel ceil decreased with the distance from the fire source, and greater

fire power always has a higher smoke temperature. According to the smoke temperature variation tendency in Fig. 2, vault smoke temperature distribution can be divided into two regions: (1) region 1 close to fire source top. Due to sudden smoke flow energy and entrainment of abundant environmental air, internal jump occurs (Kunsch 1998, LH *et al.* 2005) under three fire powers 10MW (case 1), 20MW (case 9) and 30MW (case 18), the maximum smoke temperatures drop quickly from 566°C, 995°C and 1295°C to 243°C, 420°C and 544°C, respectively. (2) one-dimension free spreading region 2. Smoke temperature declines slowly after internal jump, which can be described by Eq. (1) as below.

$$\frac{\Delta T_x}{\Delta T_{max}} = K_1 e^{-K_2(x/H)} \quad (21)$$

Where  $K_1$  is an empirical constant showed energy loss coefficient caused by internal jump. According to previous researches (Li and Ingason 2011; Oka *et al.* 2013; Hu *et al.* 2006; Kurioka *et al.* 2003) the maximum temperature  $\Delta T_{max}$  at vault of Region 1 is closely related with fire power. Therefore, it were fitted based on the following Eq. (22). Fitting results

are shown in Fig. 3.

$$\frac{\Delta T_{\max}}{T_0} = aQ^{*b} \quad (22)$$

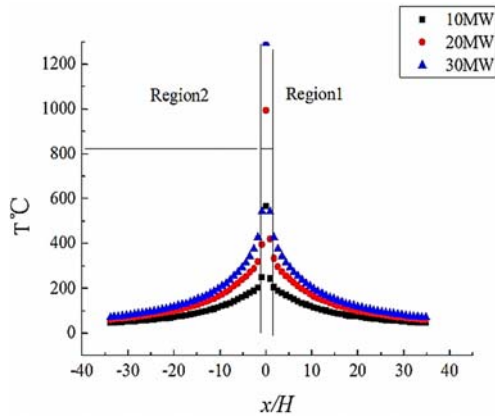


Fig. 2. Free spreading smoke temperature distribution.

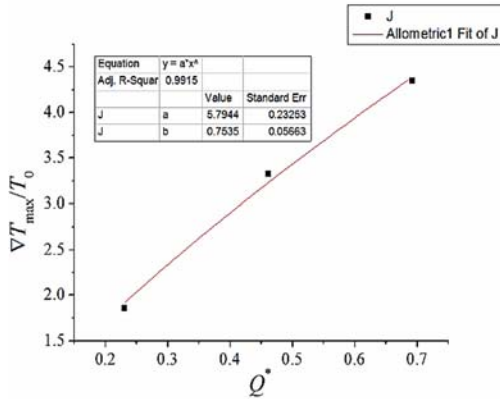


Fig. 3. Relationship between the maximum temperature at tunnel vault and fire power.

So the maximum smoke temperature coefficient at vault ( $a$ ) was calculated 5.79 and the growth factor  $b$  was 0.75.  $b$  is close to 2/3 of characteristic fire power in previous studies (Oka *et al.* 2013, Hu *et al.* 2006, 1995). Bring it into the Eq. (22)

$$\frac{\Delta T_{\max}}{T_0} = 5.79Q^{*0.75} \quad (23)$$

The flue gas temperature attenuation coefficient  $K_2$  is related with fire power and tunnel size. Smoke temperature decline distribution under different fire powers in Region 2 in Fig. 2 was fitted with Eq. (21) (Fig. 4). Fitting results are listed in Table 4. Fitting correlation coefficient is higher than 95% and  $K_1$  changes slightly, which determines the mean 0.375. However,  $K_2$  increases with the increase of fire power. According to Hu's free smoke spreading decline formula (Hu and Chow 2008),  $K_2 \propto m$ ,  $m \propto Q^{*1/3}$ , indicating that  $K_2$  is related with 1/3 power of characteristic fire power. Its fitting results are shown in

$$K_2 = aQ^{*1/3} + b \quad (24)$$

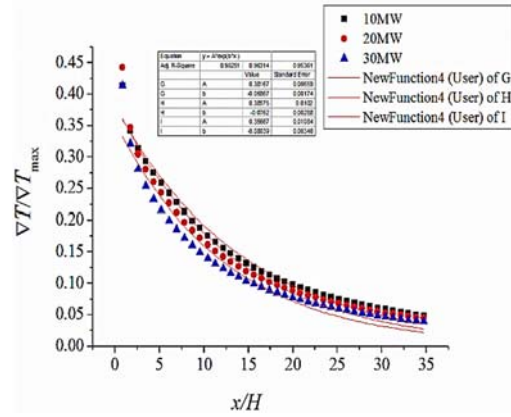


Fig. 4. Smoke temperature decline in tunnel under different fire powers.

Table 4 Fitting coefficient of smoke temperature decline

Fire power (MW)	Characteristic fire power	$K_2$	$K_1$	Correlation coefficient
10	0.231	0.068	0.365	0.98
20	0.461	0.076	0.382	0.963
30	0.692	0.082	0.385	0.953

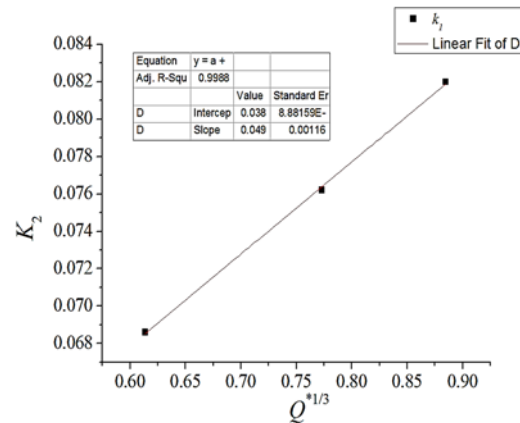


Fig. 5. Variation of  $K_2$  with fire power.

$$It\ can\ be\ seen\ from\ K_2 = 0.049Q^{*1/3} + 0.038 \quad (25)$$

Bring Eq. (23),  $K_1$  and  $K_2$  into Eq. (21) and the free spreading smoke temperature decline formula would be known:

$$\Delta T_x = 2.17Q^{*0.75}T_0e^{-(0.049Q^{*1/3} + 0.038)x/H} \quad (26)$$

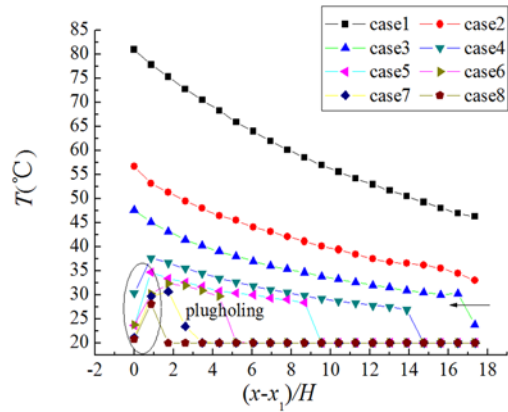
#### 4.2 Smoke Temperature Distribution in Non-Smoke Evacuation Region

Smoke temperature decline distributions in the non-smoke evacuation region under different fire powers and smoke exhaust rates are shown in Fig. 6. It can be seen that under small smoke exhaust rate, smoke temperature distributes continuously and reduces gradually with the increase of spreading distance

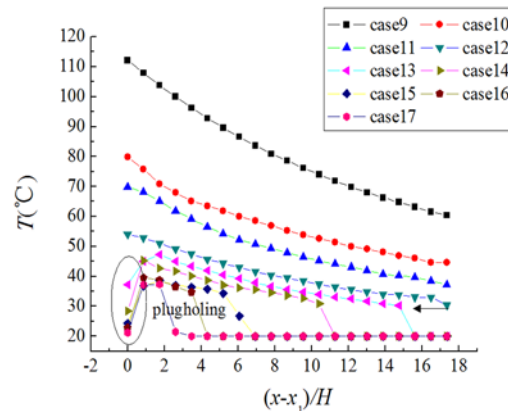
and what is more, the smoke temperature under smaller exhaust rate is always higher. No matter what fire power it is, smoke temperature underneath the smoke vent drops suddenly and is lower than smoke temperature behind smoke vent, when smoke exhaust rate increases to a certain value (smoke exhaust rates in Fig. 6 are case 4: 10MW, 3.66m/s; case 13: 20MW, 4.88 m/s; case 23: 30MW, 6.11 m/s). At the same time, temperature at the tunnel exit drops to ambient temperature suddenly, indicating that smoke spreading begins to be controlled inside the tunnel. In Fig. 6(b), when fire power is 20MW and smoke exhaust rate is smaller than 4.88 m/s (case9~case12), smoke temperature distributes continuously, but it begin to show step changes when smoke exhaust rate exceeds 4.88 m/s (case13~case17). This is because plug-holing appears when the exhaust rate is large enough. Smoke temperature behind the smoke vent is higher than that underneath the smoke vent. Given fixed fire power, smoke will form a certain thick smoke layer on the tunnel vault. Driven by smoke exhaust fans, this smoke layer will flow into the discharge flue. Smoke layer underneath the smoke vent thins gradually as smoke exhaust rate increases until plug-holing appears. At this moment, temperature below the smoke vent is the temperature of mixed fresh air and some smoke, which is close to ambient temperature. On the other hand, abundant fresh air will be extracted from the tunnel after plug-holing. Fresh air inflow from the tunnel entrance will increase ventilation velocity at tunnel entrance and hinder smoke spreading, thus inhibiting smoke within the tunnel.

Variation of spreading distance with smoke exhaust rate is shown in Fig. 7. Smoke spreading distance under different fire powers can be divided into three stages according to the variation tendency. This was explained by taking the example of 20MW fire power. In the first stage (smoke exhaust rate < 3m/s), smoke spreading distance remains basically same as the smoke exhaust rate increases, implying that this smoke exhaust rate couldn't control smoke spreading and smoke will still spread to tunnel exit. No plug-holing was observed underneath the smoke vent and only high-temperature smoke is discharged from the tunnel. Smoke temperature drops quickly with the increase of smoke exhaust rate. This stage can be called the heat exhaust stage. In the second stage (3m/s < smoke exhaust rate < 6m/s), smoke spreading distance decreases significantly. Smoke backflow distance reduces sharply with the increase of smoke exhaust rate and plug-holing begins to occur underneath the smoke vent (case13~case17). This stage is called smoke backflow stage. In the third stage (smoke exhaust rate > 6m/s), smoke spreading distance reduces slightly and smoke in the non-smoke evacuation region behind the smoke vent could be viewed controlled completely. This stage is called full smoke exhaust stage. Smoke spreading distances under different fire powers were compared, finding that smoke spreading distance in the second and third stages could be reduced to about 5 times that of tunnel height (5H). Therefore, the smoke exhaust rate when smoke backflow distance is controlled at

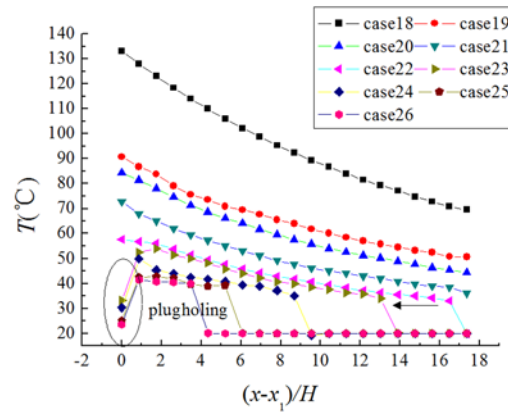
5H away from the smoke vent was viewed as complete effective smoke exhaust rate. This is a little different from the small-scale experimental result (4H) of Vauquelin and Telle (2005). This is because O.Vauquelin made a small-scale experiment and smoke vent layout was different from the actual tunnel model in this paper. Hence, it suggested to regard smoke is controlled completely when fire power in actual tunnel is 10MW, 20MW and 30MW. The corresponding smoke exhaust rates are at least 100 m<sup>3</sup>/s, 120 m<sup>3</sup>/s and 140 m<sup>3</sup>/s.



a) 10MW



b) 20MW



c) 30MW

**Fig. 6. Temperature distribution in the non-smoke evacuation region.**

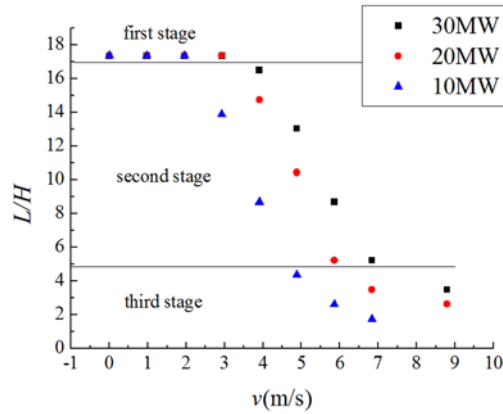


**Fig. 7. Variation of smoke spreading distance behind the smoke vent with smoke exhaust rate.**

### 4.3 Maximum Smoke Temperature Model in the Non-Smoke Evacuation Region

The maximum smoke temperature is related with smoke exhaust rate and fire power. The relation between maximum smoke temperatures in the non-smoke evacuation region and smoke exhaust rate are presented in Fig. 8. Under the same smoke exhaust rate, the maximum smoke temperature increase with fire power. With the increase of smoke exhaust rate, the maximum smoke temperature decreases gradually. Such reduction slows down continuously. To explore relations between the maximum smoke temperature and fire power as well as smoke exhaust rate, the smoke temperature was adimensionalized:

$$\Delta T_{v, \text{dimensionless}} = \frac{T_{v, \text{max}} - T_0}{T_{v_0, \text{max}} - T_0} = \frac{\Delta T_{v, \text{max}}}{\Delta T_{v_0, \text{max}}} \quad (27)$$

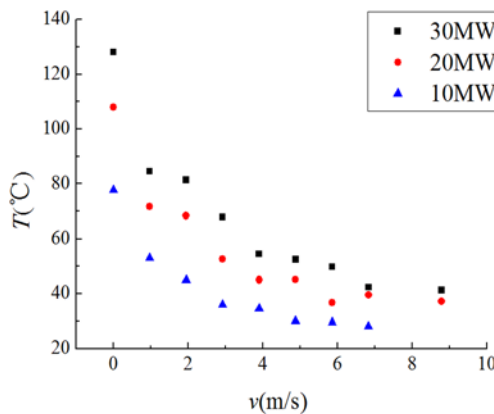


**Fig. 8. Maximum smoke temperature in the non-smoke evacuation region under different smoke exhaust rates.**

Where  $T_{v, \text{max}}$  is the maximum smoke temperature in the non-smoke evacuation region when smoke exhaust rate is  $v$  and  $T_{v_0, \text{max}}$  is the maximum smoke temperature in the non-smoke evacuation region when smoke exhaust rate is 0. Fig. 9 shows variation of the dimensionless maximum smoke temperature in the non-smoke evacuation region against smoke

exhaust rate. Logarithmic fitting between dimensionless smoke temperature under different fire powers and smoke exhaust rate is shown in Fig. 10. The fitting formula is:

$$\frac{\Delta T_{v, \text{max}}}{\Delta T_{v_0, \text{max}}} = Ae^{-K_3 v^*} + B \quad (28)$$

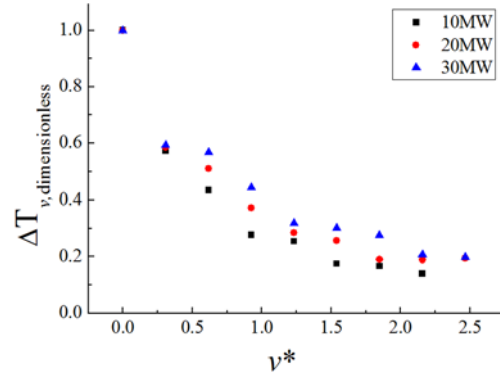


**Fig. 9. Dimensionless maximum smoke temperature in the non-smoke evacuation region under different smoke exhaust rates.**

Where  $A, B$  are fitting coefficients (Table 5) and  $K_3$  are maximum smoke temperature decline coefficient with smoke exhaust rate.

**Table 5 Fitting coefficients under different fire powers**

Characteristic fire power ( $Q^*$ )	$K_3$	$A$	$B$	Correlation coefficient
0.231	2.38	0.8	0.185	0.99
0.461	2.016	0.81	0.19	0.965
0.692	1.74	0.805	0.195	0.958

It can be seen from Table 5 that fitting coefficient under all fire powers is higher than 95%. But  $A$  and  $B$  changes slightly, which could be viewed as constants. Here, they were set the mean of three fire powers:  $A=0.81$  and  $B=0.19$ . Fire power mainly influences temperature decline coefficient  $K_3$ ,  $K_3$  decreases from 2.38 to 1.74 when fire power increases from 10MW to 30MW, indicating the slow temperature decline. Therefore,  $K_3$  was taken as the function of fire power for linear fitting ( $K_3 = 2.685 - 1.39Q^*$ ) (29)

Substitute Eq.(29) and  $A, B$  into Eq.(28), and the maximum smoke model in the non-smoke evacuation region is gained:

$$\frac{\Delta T_{v, \text{max}}}{\Delta T_{v_0, \text{max}}} = 0.81e^{-(2.685 - 1.39Q^*)v^*} + 0.19 \quad (30)$$

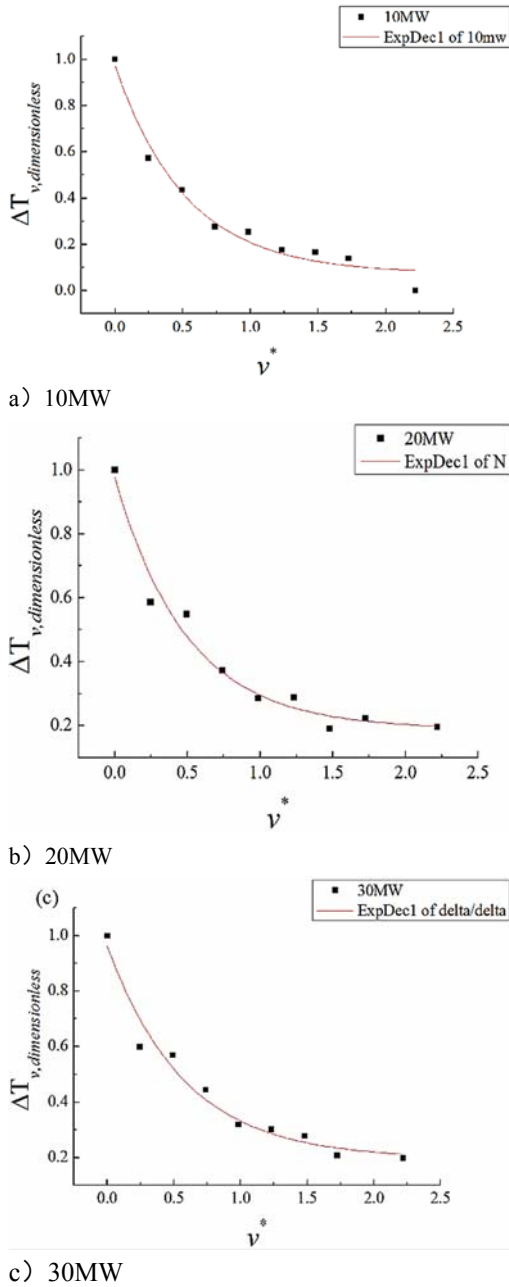


Fig. 10. Logarithmic fitting results of dimensionless temperature and smoke exhaust rate.

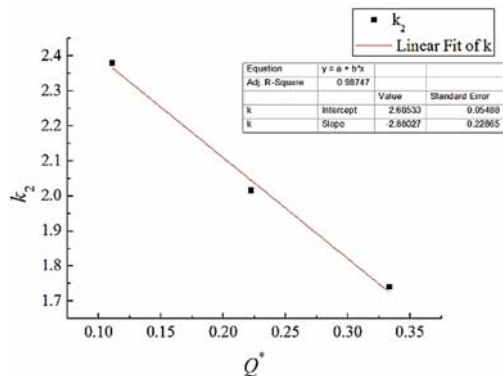


Fig. 11. Linear fitting of  $K_2$ .

Combine Eq. (26) and (30), the semi-empirical formula of the maximum smoke temperature in the non-smoke evacuation region of semi-traverse ventilation tunnel can be obtained:

$$\frac{\Delta T_{v,max}}{T_0} = 2.17Q^{0.75}e^{-(0.049Q^{2/3} + 0.038)(x/H)} \bullet (0.81e^{-(2.685-1.39Q^*)v^*} + 0.19) \quad (31)$$

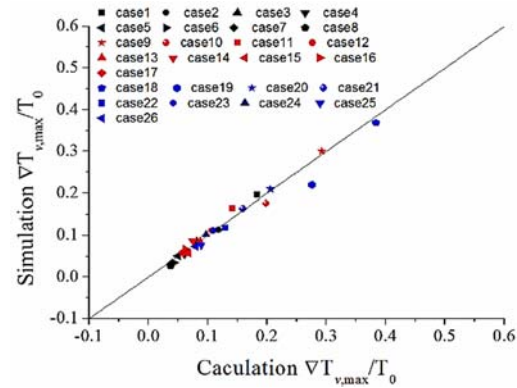
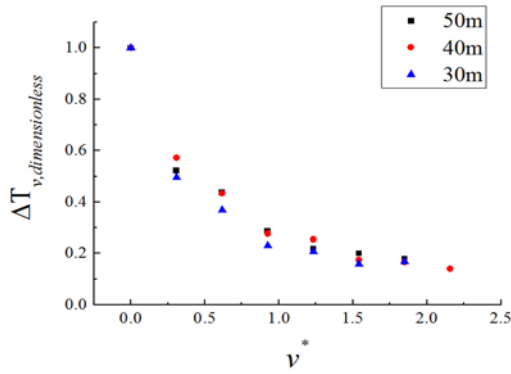


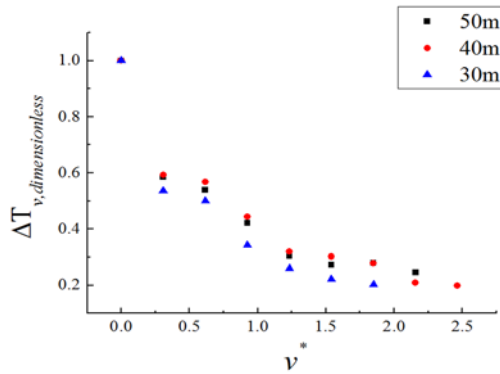
Fig. 12. Comparison of simulated results and calculated results.

#### 4.4 Effect of Smoke Vent Interval on Smoke and Heat Exhaust Efficiency

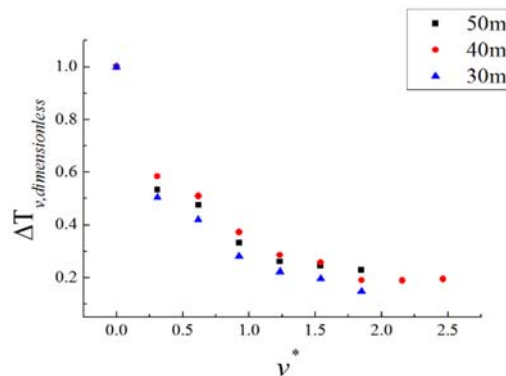
To study effect of smoke vent interval on maximum smoke temperature in the non-smoke evacuation region, smoke vents were installed at different intervals by using same method of the original interval (40m). Variation of the dimensionless maximum smoke temperature in the non-smoke evacuation region against characteristic smoke exhaust rates is shown in Fig. 13 (fire power is same). When smoke vent interval is 40m, the maximum temperature is high, indicating the low smoke and heat exhaust efficiency. This is because smoke and heat exhaust efficiency of semi-traverse ventilation system (the ratio of smoke heats flowing into the discharge flue and fire power) is related with smoke temperature flowing into smoke vent and flow rate. Under small smoke vent interval, temperature of smoke which flows into smoke vent which is close to the fire source is relative high and the smoke vent has good smoke and heat exhaust efficiency. If smoke vent interval increases, the smoke vent is far away from the fire source and temperature of smoke that flows into the smoke vent decreases, which deteriorates smoke and heat exhaust efficiency. With the further increasing of smoke vent interval, smoke and heat exhaust efficiency further increases, because smoke inflow into the smoke vent close to the exhaust fan increases. But it observed from Fig. 13 that smoke vent interval influences smoke temperature slightly and the maximum temperature difference is smaller than 10°C. Therefore,  $x$  can be calculated from Eq.(31), valuing 85m, 105m and 130m when the smoke vent interval is 30m, 40m and 50m, respectively. Calculated results were compared with simulated ones.



a) 10MW



b) 20MW



c) 30MW

**Fig. 13. Variation of maximum temperature with smoke exhaust rate under different smoke vent intervals.**

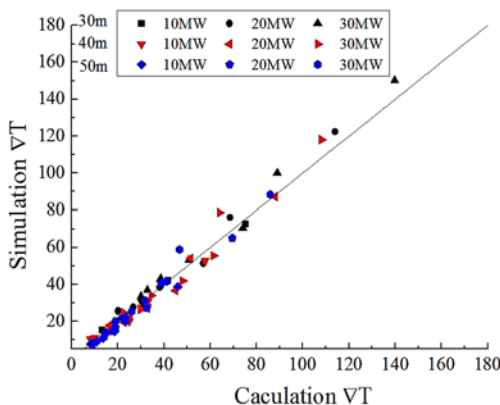


**Fig. 14. Comparison of simulated results and calculated results.**

## 5 CONCLUSIONS

In this paper, a full-scale semi-traverse ventilation tunnel model is established by using FDS numerical simulation to study smoke temperature distribution in the non-smoke evacuation region under different smoke exhaust rates. Relationship between the maximum smoke temperature and smoke exhaust rate is explored. Based on simulated results and dimensionless analysis, a maximum smoke temperature model in the non-smoke evacuation region which is related with fire power and smoke exhaust rate is established. It mainly concludes that:

- (1) Under small smoke exhaust rate, smoke temperature distributes continuously in the tunnel and decreases with the increase of spreading distance. Smoke spreading distance can be divided into three stages according to changes of smoke exhaust rate: heat exhaust stage, smoke backflow stage and full smoke exhaust stage. When smoke exhaust rate increases to a certain value, plug-holing occurs below the smoke vent (10MW, 60m<sup>3</sup>/s; 20MW, 80 m<sup>3</sup>/s; 30MW, 100 m<sup>3</sup>/s). Temperature below the smoke vent and tunnel exit drop sharply, while smoke spreading is controlled within the tunnel.
- (2) The maximum smoke temperature in the non-smoke evacuation region increases with the increase of fire power, but reduces with the increase of smoke exhaust rate. Such reduction slows down as smoke exhaust rate increases, but accelerates as fire power increases.
- (3) A maximum smoke temperature model (formula) in the non-smoke evacuation region is proposed according to simulated results and dimensionless analysis. It shows that the dimensionless maximum smoke temperature is proportional to 0.75 power of dimensionless fire power, and attenuates exponentially with the increase of smoke exhaust rate. The attenuation coefficient is inversely proportional to dimensionless fire power.
- (4) Smoke vent interval mainly influences  $\Delta T_{v_0, max}$ , but affects  $\Delta T_{v, adimensionalized}$  slightly. Eq.(31) is also application to ventilation tunnels with different smoke vent intervals.
- (5) Smoke exhaust efficiency of semi-traverse mechanical ventilation system is also related with smoke vent shape, tunnel shape and fire source position. Therefore, Eq.(31) has certain limitation. This paper mainly focuses on the maximum smoke temperature and smoke spreading characteristics in the non-smoke evacuation region of semi-traverse ventilation tunnel through numerical simulation. Related conclusions need more experimental supports.

## ACKNOWLEDGMENTS

This work was funded by the Natural Science Foundation of Guangdong Province in China under

Grant Number S2013010016748 and Guangdong Province Key Laboratory of Efficient and Clean Energy Utilization (2013A061401005), South China University of Technology

## REFERENCES

- Ballesteros Tajadura, R., C. Santolaria Morros and E. Blanco Marigorta (2006). Influence of the slope in the ventilation semi-transversal system of an urban tunnel. *Tunnelling and Underground Space Technology incorporating Trenchless Technology Research* 21, 21-28.
- Brahim, K., B. Mourad, E. C. Afif and B. Ali (2013). Control of smoke flow in a tunnel. *JAFM* 6(1), 46-60.
- Choi, J. S. (2005). Experimental Investigation on Smoke Propagation in a Transversely Ventilated Tunnel. *Journal of Fire Sciences* 23, 469-483.
- Chow, W. K. and J. Li (2011). On the bidirectional flow across an atrium ceiling vent. *Building and Environment*, 46, 2598-2602.
- Chow, W. K. and Y. Gao (2009). Oscillating behaviour of fire-induced air flow through a ceiling vent. *Applied Thermal Engineering* 29, 3289-3298.
- Fan, C. G., J. Ji, Z. H. Gao, J. Y. Han and J. H. Sun (2013). Experimental study of air entrainment mode with natural ventilation using shafts in road tunnel fires. *International Journal of Heat and Mass Transfer* 56, 750-757.
- Harish, R. and K. Venkatasubbaiah (2014). Effects of buoyancy induced roof ventilation systems for smoke removal in tunnel fires. *Tunnelling and Underground Space Technology* 42, 195-205.
- He, Y. (1999). Smoke temperature and velocity decays along corridors. *Fire Safety Journal* 33, 71-74.
- Hu, L. H., J. W. Zhou, R. Huo, W. Peng and H. B. Wang (2008). Confinement of fire-induced smoke and carbon monoxide transportation by air curtain in channels. *Journal of Hazardous Materials* 156, 327-334.
- Hu, L. H., R. Huo and W. K. Chow (2008). Studies on buoyancy-driven back-layering flow in tunnel fires. *Experimental Thermal and Fluid Science* 32, 1468-1483.
- Hu, L. H., R. Huo, W. K. Chow, H. B. Wang and R. X. Yang (2004). Decay of buoyant smoke layer temperature along the longitudinal direction in tunnel fires. *Journal of Applied Fire Science* 13, 53-77.
- Hu, L. H., R. Huo, W. Peng, W. K. Chow and R. X. Yang (2006). On the maximum smoke temperature under the ceiling in tunnel fires. *Tunnelling and Underground Space Technology* 21, 650-655.
- Hu, L. H., W. Peng and R. Huo (2008). Critical wind velocity for arresting upwind gas and smoke dispersion induced by near-wall fire in a road tunnel. *Journal of Hazardous Materials* 150, 68-75.
- Jafari, M. J., A. Karimi, A. E. Usachov and H. Kanani Moghaddam (2011). The fire simulation in a road tunnel. *JAFM* 4(1), 121-138.
- Ji, J., Z. H. Gao, C. G. Fan, W. Zhong and J. H. Sun (2012). A study of the effect of plug-holing and boundary layer separation on natural ventilation with vertical shaft in urban road tunnel fires. *International Journal of Heat and Mass Transfer* 55, 6032-6041.
- Jie, J., L. Kaiyuan, Z. Wei and H. Ran (2010). Experimental investigation on influence of smoke venting velocity and vent height on mechanical smoke exhaust efficiency. *Journal of Hazardous Materials* 177, 209-215.
- Kashef, A., Z. Yuan and B. Lei. (2012). Some effects on natural ventilation system for subway tunnel fires. *In Proceedings from the Fifth International Symposium on Tunnel Safety and Security* 309-318.
- Kunsch, J. P. (1998). Critical velocity and range of a fire-gas plume in a ventilated tunnel. *Atmospheric Environment* 33, 13-24.
- Kurioka, H., Y. Oka, H. Satoh and O. Sugawa (2003). Fire properties in near field of square fire source with longitudinal ventilation in tunnels. *Fire Safety Journal* 38, 319-340.
- Lee, S. R. and H. S. Ryou (2006). A numerical study on smoke movement in longitudinal ventilation tunnel fires for different aspect ratio. *Building and Environment* 41, 719-725.
- Hu, L. H., R. Huo, L. Y. Zhou, H. B. Wang and W. K. Chow (2005). Full scale burning tests on studying smoke temperature and velocity along a corridor. *Tunnelling and Underground Space* 20, 223-229.
- Li, L., X. Cheng, Y. Cui, S. Li and H. Zhang (2012). Effect of blockage ratio on critical velocity in tunnel fires. *Journal of Fire Sciences* 30, 413-427.
- Li, Y. Z., B. Lei and H. Ingason (2011). The maximum temperature of buoyancy-driven smoke flow beneath the ceiling in tunnel fires. *Fire Safety Journal* 46, 204-210.
- Lin, C. and Y. K. Chuah (2008). A study on long tunnel smoke extraction strategies by numerical simulation. *Tunnelling and Underground Space Technology* 23, 522-530.
- Lin, P., S. M. Lo and T. Li (2014). Numerical study on the impact of gradient on semi-transverse smoke control system in tunnel. *Tunnelling and Underground Space Technology* 44, 68 - 79.
- McCaffrey, B. J. and J. G. Quintiere. 1977. *Buoyancy driven countercurrent flows generated by fire source*. Washington USA.

- McGrattan, K. (2006). Fire Dynamics Simulator (Version 4) Technical Reference Guide, NIST Special Publication 1018.
- McGrattan, K. B., H. R. Baum and R. G. Rehm (1998). Large Eddy simulations of smoke movement. *FIRE SAFETY JOURNAL* 30, 161-178.
- Oka, Y., N. Kakae, O. Imazeki and K. Inagaki (2013). Temperature Property of Ceiling Jet in an Inclined Tunnel. *Procedia Engineering* 62, 234-241.
- Vauquelin, O. and D. Telle (2005). Definition and experimental evaluation of the smoke confinement velocity in tunnel fires. *Fire Safety Journal* 40, 320-330.
- Vauquelin, O. and M. O (2002). Smoke extraction experiments in case of fire in a tunnel. *Fire Safety Journal* 37, 525-533.
- Vauquelin, O. and W. Y (2006). Influence of tunnel width on longitudinal smoke control. *Fire Safety Journal* 41, 420-426.
- Wang, Y., J. Jiang and D. Zhu (2009). Full-scale experiment research and theoretical study for fires in tunnels with roof openings. *FIRE SAFETY JOURNAL* 44, 339-348.
- Xu, Q., L. Yi, Z. Xu and D. Wu (2013). Preliminary Study on Exhaust Efficiency of Smoke Management System in Tunnel Fires. *Procedia Engineering* 52, 514-519.
- Yi, L., R. Wei, J. Peng, T. Ni, Z. Xu and D. Wu (2015). Experimental study on heat exhaust coefficient of transversal smoke extraction system in tunnel under fire. *Tunnelling and Underground Space Technology* 49, 268-278.
- Zhang, Q., X. Guo, E. Trussoni, G. Astore, S. Xu and P. Grasso (2012). Theoretical analysis on plane fire plume in a longitudinally ventilated tunnel. *Tunnelling and Underground Space Technology* 30, 124-131.